Practical improvements of modelling of photoacoustic Helmholtz cells

Tomasz Starecki*

Institute of Electronic Systems, Warsaw University of Technology,
Nowowiejska 15/19, 00-665 Warsaw, Poland

ABSTRACT

The paper presents some improvements to the transmission line model of photacoustic Helmholtz cell. The improvements were aimed to obtain much better agreement between theoretical and practical values of Q-factors of the cells, and were based on measurements of number of cells and comparison of measurement results with theoretical frequency responses. The measured cells had dimensions typical for photoacoustic setups.

Keywords: photoacoustics, Helmholtz cell, improved transmission line model

1. INTRODUCTION

From among many different kinds of photoacoustic cells, the one that is very often used is Helhmoltz resonator.[1-3] Such a cell consists of two cavities connected with a capillary (fig. 1). Properties of a photoacoustic cell have direct impact on the overall properties of the whole photoacoustic setup - in particular on its sensitivity. This means that such a cell should be design carefully. In order to shorten time of development and examine properties of the cell before it is manufactured, thus being able to improve the design before its practical implementation, computer simulation tools are commonly used. However, in case of Helmholtz structure this introduce some problems.

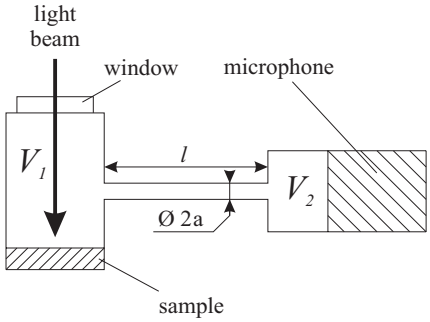

Fig. 1. Structure of a photoacoustic Helmoltz cell.

2. MODELLING OF PHOTOACOUSTIC HELMHOLTZ CELLS

The most common technique of simulations of photoacoustic Helmholtz cells is acousto-electrical analogies.[4-6] Such an approach requires that every acoustical element of the structure being analysed is replaced by its electrical counterpart. As a result Helmholtz structure can be modelled by a circuit diagram based on lumped constants components (fig. 2a) in which capacitors simulate cavities, while series connection of an inductor and resistor is to reflect acoustical properties of the duct connecting the cavities. The problems arrive already at the level of expressions defining behaviour of the L, and R components, as different authors use different sets of definitions.[4] However the main issue is that none of these definitions works well, as calculated Q-factors of the cells are very often number of times (20 to over 1000 times) greater than practical values verified by measurements.[4,7]

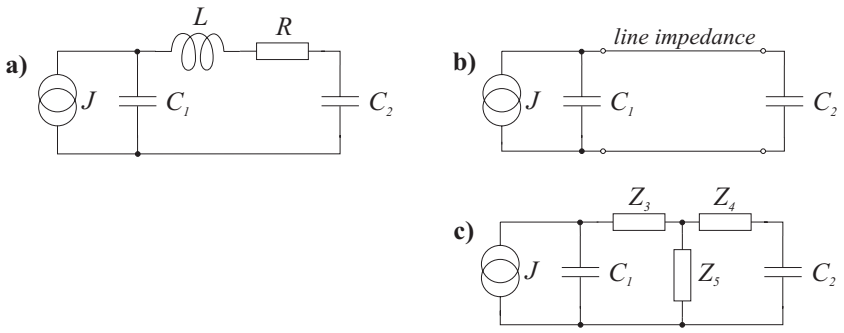

Fig. 2. Electric models of photoacoustic Helmholtz cell: a) lumped components model, b) transmission line model, c) transmission line model after conversion of the line into T-section.

*tomi@ise.pw.edu.pl

A model which gives much closer evaluation of loss mechanisms, due to better representation of viscous and thermal properties of the gas filling the chamber, is a transmission line model (fig. 2b). In this model the duct between the cavities is replaced by a transmission line. Usually it is being stated that such an approach should be used only when size of the acoustical component is at the same (or greater) order of magnitude as acoustical wavelength. However in case of photoacoustic Helmholtz cells transmission line model gives much better results than the lumped components model even in case of very short ducts.

In the mentioned transmission line model, characteristic impedance Z_w and propagation constant Γ_w of the line are defined as follows:[8]

$$Z_w = \sqrt{\frac{R + j\omega L}{G + j\omega C}}, \qquad \Gamma_w = \sqrt{(R + j\omega L)\,(G + j\omega C)}, \tag{1}$$

where:

$$R + j\omega L = j\,\frac{\omega\rho}{\pi a^2 (1 - F_v\, e^{j\Phi_v})}, \tag{2}$$

$$G + j\omega C = j\,\frac{\omega\pi a^2}{\rho c^2}\,[1 + (\kappa - 1)\,F_t\, e^{j\Phi_t}]. \tag{3}$$

Symbol κ in the above expressions denotes adiabate coefficient of the gas ($\kappa = c_p / c_v$), while function F is defined as:

$$F_{v,t}\, e^{j\,\Phi_{v,t}} = \frac{2\,J_1(\sqrt{-j}\,r_{v,t})}{\sqrt{-j}\,r_{v,t}\,J_0(\sqrt{-j}\,r_{v,t})}, \tag{4}$$

where J_0 and J_1 are complex Bessel functions of the zero and first order. Symbols v and t in the equations (2) and (3) indicate which of the r_v and r_t variables should be used in place of r in the equation (4):

$$r_v = a\sqrt{\frac{\omega\rho}{\eta}}, \qquad r_t = a\sqrt{\frac{\omega\rho c_p}{\lambda}}. \tag{5}$$

Symbols used in the given expressions denote:

a - radius of the capillary (duct connecting the cavities),
c_p - heat capacity of the gas,
c_v - volume capacity of the gas,
ρ - mass density of the gas,
λ - thermal conductivity of the gas,
η - viscosity of the gas.

The transmission line defined above can be easily converted into equivalent T-section (fig. 2c) in which the impedances Z_3, Z_4 and Z_5 are defied as: [9]

$$Z_3 = Z_4 = Z_w \tanh\frac{\Gamma_w\, l}{2}, \qquad Z_5 = \frac{Z_w}{\sinh(\Gamma_w\, l)}, \tag{6}$$

where l denotes length of the duct. Values of the capacitors C_1 and C_2 from fig. 2 are defined by the expression:[10]

$$C_i = \frac{V_i}{\rho c^2}, \tag{7}$$

where:

V_i - volumes of the cavities,
c - speed of sound in the gas filling the chamber.

3. IMPROVED TRANSMISSION LINE MODEL

Although transmission line model based on the above definitions gives much better fit to practical values of Q-factor of photoacoustic Helmholtz cells, quality of the model is still unacceptable for many applications. Because, although errors of Q-factor evaluations based on such a model are approximately one order of magnitude smaller in comparison to the best lumped components model, still in some cases calculated values of Q-factor of the cells are over 10 times greater than the measured ones. Such a situation suggests that there must be some additional loss mechanism in the cells which is not included in existing models. In order to include some additional effects (in particular loss mechanisms), the transmission line model was substantially enhanced (fig. 3). Additional components in the enhanced model included radiation loss R_{rad}:[11]

$$R_{rad} = \frac{\rho\omega^2}{2\pi c} , \tag{8}$$

and end corrections L_{ends}, R_{ends} (valid for circular cross-section of the interconnecting duct) that can be evaluated as:[11]

$$R_{ends} = \frac{\sqrt{8\rho\omega\eta}}{\pi a^2} , \qquad L_{ends} = \frac{16\rho}{3\pi a^2} . \tag{9}$$

(Other evaluations of the inductive component of the end correction that can be found in literature[12] differ from the one given above not more than a few tens percent, and do not have significant impact on the final shape of the simulated frequency response of the cell.)

Acoustical impedance of the microphone Z_{micr}, which is also responsible for some losses, depends strongly on the microphone design, and its evaluation is a relatively complex problem. Measurements of the cell responses for the purpose of this work were done with B&K 4134 condenser microphone. Calculations performed according to the analysis presented by Zukerwar [13] gave results indicating that disturbances introduced to the investigated cells by the mentioned microphone were small enough to be completely neglected in the simulations.

It should be noted, that values of the capacitors C_1 and C_2 is not constant. Capacitance equivalent to the effective volume of the cavities can be described as: [11]

$$C_i(\omega) = C_i \, (\kappa - 2 \, (\kappa - 1) \, Re(\Psi(a_i \sqrt{j\frac{\omega c_p}{\eta}}))) , \tag{10}$$

where:

$$\Psi(z) = \frac{1}{2} - \sqrt{-j}\frac{J_1(z)}{|z|J_0(z)} . \tag{11}$$

In case of microphone cavity, equivalent volume of the microphone C_{Vmicr} should be also taken into account.

Viscous losses of the cavities R_{vCi} can be calculated from: [11]

$$R_{vCi}(\omega) = \frac{R_t a_i^2 \omega\rho}{48\eta} \, Im\left(\frac{1}{\Psi(a_i \sqrt{j\frac{\omega\rho}{\eta}})}\right) , \tag{12}$$

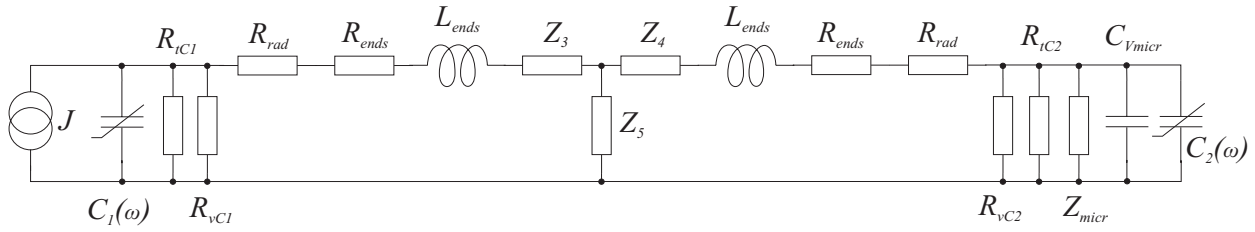

Fig. 3. Enhanced transmission line model of photoacoustic Helmholtz cell including some additional loss sources.

where a_i is radius of the cavity (assuming that the cavities have cylindrical shape), and R is defined as:

$$R_i = \frac{8\pi\eta l_i}{\pi a_i^2}, \tag{13}$$

where l_i is the cavity length.

Bottom limit of the thermal cavity losses R_{tCi} can be evaluated as: [11]

$$R_{tCi} = \frac{1}{3} G_i(\omega) L_i^2(\omega) \omega^2 , \tag{14}$$

in which:

$$G_i(\omega) = 2C_i \omega (1 - \kappa) Im(\Psi(a_i \sqrt{j\frac{\omega c_p}{\lambda}})), \qquad L_i(\omega) = \frac{3}{8} L_i Im\left(\frac{1}{\Psi(a_i \sqrt{j\frac{\omega\rho}{\eta}})}\right), \tag{15}$$

where C_i is calculated in accordance to (7), and:

$$L_i = \frac{4\rho l_i}{3\pi a_i^2} . \tag{16}$$

The enhancements to the transmission line model described above made the model much more complex, and although slightly improved agreement with the measurements, were still far away from satisfactory results. As further work toward this direction didn't seem to be promising, another approach was chosen.

4. MEASUREMENTS AND SIMULATIONS

Relatively good agreement between theoretical results obtained from the basic transmission line model with the measurements as regards to the resonance frequencies of the cells, while having problems when coming to Q-factor evaluation, led to the idea of use of the basic transmission line model in which real parts of the impedances Z_3 and Z_4 would be increased by some correction coefficients in order to simulate higher level of losses, while leaving imaginary parts of the impedances unchanged. The software used for simulations was at first working in such a way, that after reading in measurement results and calculating simulated frequency responses of the cell, both (theoretical and measured) characteristics were being displayed. Taking into consideration that both curves were displayed in such a way that they were having common points at very low, as well as at very high, frequencies, it was easy to see any differences in the shape of resonance peak. In order to get at least some brief idea about the value of the correction coefficients, the software was modified, so that after having theoretical and measured frequency responses displayed, it was possible to manually change the correction factors (with the resolution of 1%) and get the theoretical frequency response recalculated and redraw. Thus, in a few iterations it was possible to get both displayed characteristics in relatively good agreement and store the correction factor value.

In order to have reasonable amount of experimental data for verification of the simulations, a whole set of test cells was manufactured and measured. All the cells had identical sample cavity (2.0 cm^3), the microphone cavity was produced in four sizes (0.5, 1.0, 1.5, and 2.0 cm^3), while the duct connecting the cavities had length of 2.0, 3.0 or 4.0 cm and diameter of 1.0, 2.0, 3.0 or 4.0 mm. Taking into consideration, that frequency responses of all the cells had to be measured with high accuracy and resolution, a high-resolution-measurements microprocessor system was used.[14] All 48 dimension combinations of the cell were assembled, measured and compared with simulations, resulting in a set of 48 correction factors showed in fig. 4.

It can be easily noticed from fig. 4 that correction factors increase with the duct diameter and against microphone cavity volume, while length of the duct has relatively small influence on the value of correction coefficients. This probably means that losses inside the duct are quite well simulated in the transmission line model, and the main loss not included in the model is outside of the duct. A possible cause of additional damping may be interaction of the jet flowing out from the duct into the microphone cavity with gas particles thrown out from the same jet and reflected form the microphone membrane located in small distance opposite to the duct opening. Similar problem exists at the other end of the duct if the

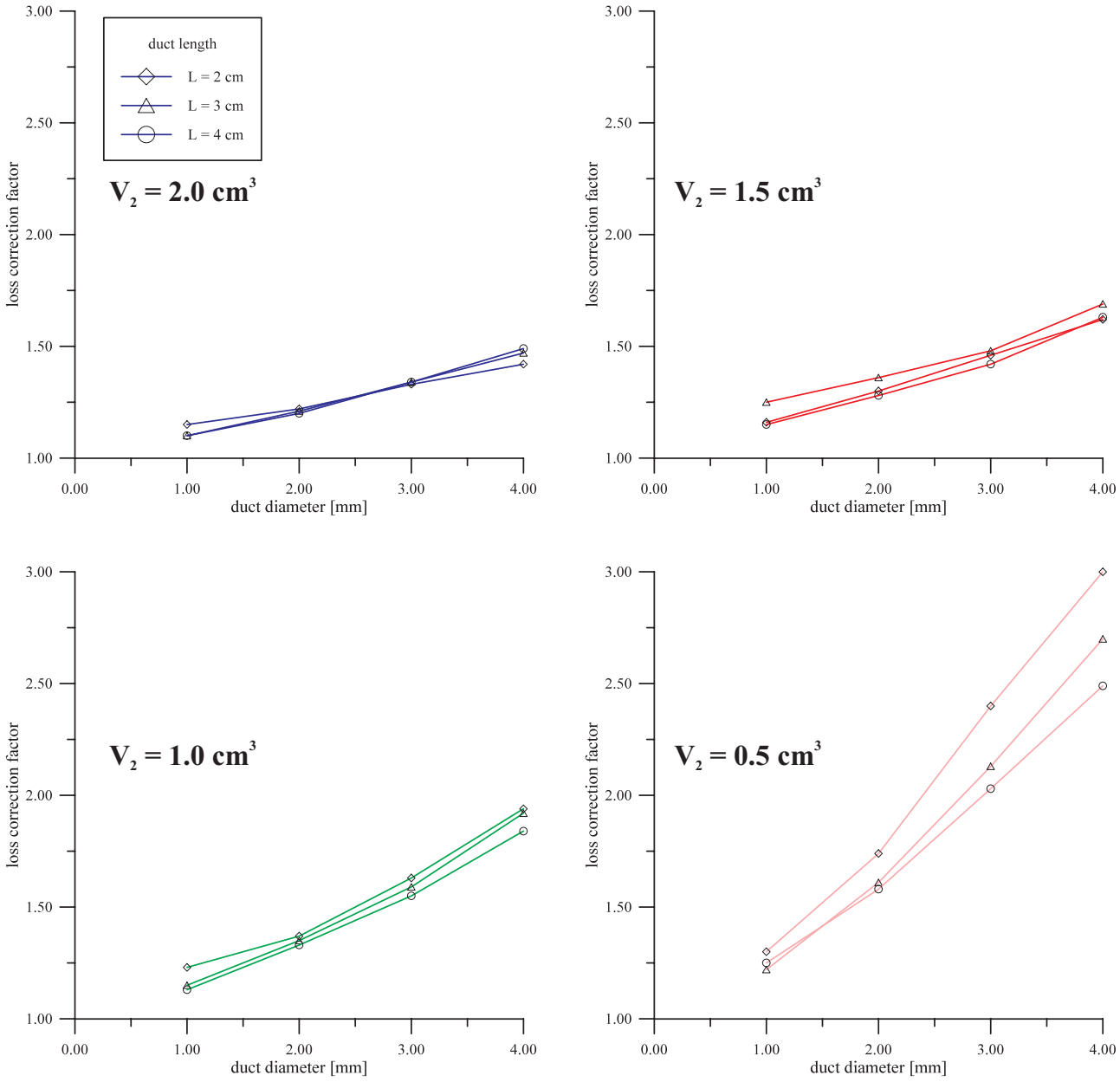

Fig. 4. Values of the loss correction coefficients vs. duct length, diameter, and microphone cavity volume.

sample cavity has small diameter. The results confirm also some earlier experiments showing that too small microphone cavity volume (0.5 - 1.0 cm^3) results in significant damping of the signal.[15] It should be also noticed, that at a given microphone cavity volume, loss correction factors vs. duct diameter show nearly linear dependance, which can be used for easy interpolation of the coefficients for other duct diameter values.

5. CONCLUSIONS

Results of the presented work show that existing electrical models of photoacoustic Helmholtz cells have unsatisfactory quality as regards to simulation of Q-factors the cells. Enhancements of the transmission line model of photoacoustic Helmholtz resonator in order to include number of different loss mechanisms discussed in literature do not

significantly improve quality of the model. In order to obtain better agreement between the transmission line model and measurements of practically implemented cells, it is possible to use another approach in which real parts of the serial impedances in T-section equivalent of the transmission line are increased by some correction factors. Quasi-linear dependence of these loss correction factors vs. duct diameter at a given microphone cavity volume, and negligible influence of the duct length on these coefficients, can be used for easy interpolation of the coefficients for intermediate duct diameter and length values.

6. REFERENCES

1. Y.-H. Pao, *Optoacoustic spectroscopy and detection*, chap. 8, Academic Press, New York, 1977.
2. A. Miklós, P. Hess, and Z. Bozóki, "Application of acoustic resonators in photoacoustic trace gas analysis and metrology", Rev. Sci. Instrum. **72**, pp. 1937-1955, 2001.
3. V. P. Zharov, and V. S. Letokhov, *Laser optoacoustic spectroscopy*, chap. 5.3, Spriger Series in Optical Sciences **37**, Springer, Berlin, Heidelberg, 1986.
4. T. Starecki, "Modelling of photoacoustic Helmholtz resonators by means of acousto-electrical analogies", Electronics and Telecommunications Quarterly **39**, pp. 307-312, 1993.
5. O. Nordhaus, and J. Pelzl, "Frequency dependence of resonant photoacoustic cells: the extended Helmholtz resonator", Appl. Phys. **25**, pp. 221-229, 1981.
6. J. Pelzl, K. Klein, and O. Nordhaus, "Extended Helmholtz resonator in low-temperature photoacoustic spectroscopy", Appl. Opt. **21**, pp. 94-99, 1982.
7. T. Starecki, *Comparative analysis of photoacoustic Helmholtz cell models* (Ph. D. thesis, in Polish), Warsaw University of Technology, Warsaw, 1994.
8. A. H. Benade, "On the propagation of sound waves in a cylindrical conduit", J. Acoust. Soc. Am. **44**, pp. 616-623, 1968.
9. F. B. Daniels, "On the propagation of sound waves in a cylindrical conduit", J. Acoust. Soc. Am. **22**, pp. 563-564, 1950.
10. P. M. Morse, *Vibration and sound*, pp. 234-235, McGraw-Hill, New York, 1948.
11. A. W. Nolle, "Small-signal impedance of short tubes", J. Acoust. Soc. Am. **25**, pp. 32-39, 1953.
12. R. W. Troke, "Tube-cavity resonance", J. Acoust. Soc. Am. **44**, pp. 684-688, 1968.
13. A. J. Zukerwar, "Theoretical response of condenser microphones", J. Acoust. Soc. Am. **64**, pp. 1278-1285, 1978.
14. T. Starecki, and M. Grajda, "Low cost miniature data acquisition and control system for photoacoustic experiments", 16th IEEE-SPIE Symposium on Photonics, Electronics and Web Engineering, Wilga 31 May - 5 June 2005 (to be published in the same conf. proceedings).
15. T. Starecki, A. Burd, S. Misiaszek, K. Opalska, M. Radtke, and M. Ramotowski, "Practical parameters of photoacoustic Helmholtz cells" (in Polish), *II Krajowa Konferencja Elektroniki, Kolobrzeg 2003* (conference proceedings) **2**, pp. 653-657, Faculty of Electronics of Koszalin University of Technology, Koszalin, 2003.